

1 A Stochastic Model for Particulate Suspension  
2 Flow in Porous Media

3 A. SANTOS and P. BEDRIKOVETSKY\*  
4 North Fluminense State University (LENEP/UENF), Brazil

5 (Received: 3 January 2003; accepted in final form: 3 April 2005)

6 **Abstract.** A population balance model for a particulate suspension transport with size  
7 exclusion capture of particles by porous rock is derived. The model accounts for particle  
8 flux reduction and pore space accessibility due to restriction for large particles to move  
9 through smaller pores – a particle is captured by a smaller pore and passes through a  
10 larger pore. Analytical solutions are obtained for a uniform pore size medium, and also  
11 for a medium with small pore size variation. For both cases, the equations for averaged  
12 concentrations significantly differ from the classical deep bed filtration model.

13 **Key words:** deep bed filtration, pore size exclusion, accessibility, stochastic model, averaging.

14 **Nomenclature**

$c$	total suspended particle concentration, $L^{-3}$ .
$C$	concentration distribution for suspended particles, $L^{-4}$ .
$f$	size distribution (probability distribution function), $L^{-1}$ .
$f_T$	size distribution of $r_s$ -particle population retained in $r_p$ -pores, $L^{-2}$ .
$h$	total vacant pore concentration, $L^{-3}$ .
$H$	concentration distribution for vacancies, $L^{-4}$ .
$J$	distribution of an $r_s$ -particle population flux per unit of cross-section area, $L^{-3} T^{-1}$ .
$\underline{J}$	distribution of an $r_s$ -particle population flux through the $r_p$ -pores per unit of cross-section area, $L^{-4} T^{-1}$ .
$k_0$	initial permeability, $L^2$ .
$k(\sigma)$	formation damage function, dimensionless.
$L$	core length, L.
$p$	pressure, $M/T^2L$ .
$P$	probability of a particle with radius $r_s$ to meet a pore with radius $r_p$ .
$r_p$	pore radius, L.
$r_s$	particle radius, L.
$t$	dimensional time, T.
15 $T$	dimensionless time.

\*Author for Correspondences: Tel: +21-24-773+6565; Fax: +21-24-773-6564;  
E-mail: pavel@lenep.uenf.br



$U$	fluid velocity, L/T.
$x$	dimensional linear co-ordinate, L.
$X$	dimensionless linear co-ordinates.
$\langle x \rangle$	average penetration depth, L.

#### Greek Symbols

$\alpha$	flux reduction factor.
$\delta$	Dirac's delta function.
$\phi$	porosity.
$\lambda'$	dimensional filtration coefficient, L <sup>-1</sup> .
$\lambda$	dimensionless filtration coefficient.
$\mu$	viscosity, ML <sup>-1</sup> T <sup>-1</sup> .
$\underline{\Sigma}(r_s, r_p)$	concentration distribution for particles with radius $r_s$ captured by pores with radius $r_p$ , L <sup>-5</sup> .
$\Sigma(r_s)$	concentration distribution for retained particles with radius $r_s$ , L <sup>-4</sup> .
$\sigma$	total deposited particle concentration, L <sup>-3</sup> .

#### Subscripts and Superscripts

0	initial value at $T = 0$ .
f	front.
p	pore/vacancy.
s	suspended (for particles).
tr	transition.
T	trapped (for retained particles).
16 (0)	boundary value at $X = 0$ .

## 17 1. Introduction

18 Deep bed filtration of water with particles occurs in several industrial and  
 19 environmental processes like water filtration and soil contamination. In  
 20 petroleum industry, deep bed filtration of drilling fluid happens during well  
 21 drilling; it also takes place near to injection wells during seawater injection  
 22 causing injectivity reduction.

23 The particle capture in porous media can be caused by different physical  
 24 mechanisms (Elimelech *et al.*, 1995):

- 25 • size exclusion (large particles are captured in small pores and pass  
 26 through large pores);
- 27 • electrical forces (London – Van der Waals, double electrical layer, etc.);
- 28 • gravity segregation;
- 29 • multi particle bridging.

30 In the current paper, the size exclusion mechanism is discussed.

31 A phenomenological model for the particle-capture and permeability-  
 32 damage process was proposed by Iwasaki (1937) and used in filtration  
 33 processes (Herzig, *et al.*, 1970) and in well injectivity with rock permeabil-  
 34 ity decline (Pang and Sharma, 1994; Wennberg and Sharma, 1997). The  
 35 model assumes linear kinetics of particle deposition, and exhibits a good



36 agreement with laboratory data. So, the model can be used for prediction  
37 purposes, like forecast of well injectivity decline based on laboratory core-  
38 flood tests. Nevertheless, the model does not distinguish between different  
39 mechanisms of formation damage. Therefore, the model cannot be used  
40 for diagnostic purposes, like determination of the dominant capture mech-  
41 anism from well data.

42 The model predicts that the particle breakthrough happens after injec-  
43 tion of one pore volume. Nevertheless, several cases where the break-  
44 through time significantly differs from one pore volume injected have been  
45 reported in the literature for particulate and polymer suspensions (Dawson  
46 and Lantz, 1972; Bartelds *et al.*, 1997; Veerapen *et al.*, 2001; Massei *et al.*,  
47 2002).

48 In case of size exclusion mechanism, the larger are the particles and the  
49 smaller are the pores, the more intensive is the capture and the larger is  
50 the formation damage. Nevertheless, several attempts to correlate the for-  
51 mation damage with sizes of particles and pores were unsuccessful (Oort *et*  
52 *al.*, 1993; Bedrikovetsky *et al.*, 2001, 2003). It could mean that either size  
53 exclusion mechanisms never dominate, or the phenomenological model for  
54 average concentrations is not general/universal enough. One of ways around  
55 this contradiction is micro scale modelling of each capture mechanism.

56 Different network micro models have been developed by Payatakes  
57 *et al.* (1973, 1974), Sahimi and Indakm (1991), Rege and Fogler (1988),  
58 (see Khilar and Fogler, 1998), Siqueira *et al.* (2003). Different physical  
59 mechanisms of particle retention are included in these models.

60 Sharma and Yortsos (1987a), derived basic population balance equations  
61 for transport of particulate suspensions in porous media. The model accounts  
62 for particle and pore size distribution variation due to different particle cap-  
63 ture mechanisms. It is assumed that an overall pore space is accessible for  
64 particles and the particle population moves with the average flow velocity  
65 of the carrier water. In the case of porous medium with the uniform pore  
66 size distribution, this assumption results in independent deep bed filtration  
67 of different particle size populations. Nevertheless, during deep bed filtration  
68 with size exclusion mechanism, particles smaller than the pore radii should  
69 pass the rock without being captured and particles larger than the pore radii  
70 should not enter the rock.

71 The pore size exclusion supposes that the particles can enter just  
72 larger pores, i.e. only the fraction of porosity is accessible for particles.  
73 Therefore, the particles are carried by water flowing just via the accessible  
74 pore space, i.e. the water flux carrying particles of a fixed size is just a frac-  
75 tion of the overall water flux via porous media. The effects of porous space  
76 accessibility and flux reduction due to finite size of polymer molecules have  
77 been observed and mathematically described for flow of polymer solutions  
78 in rocks (Dawson and Lantz, 1972; Bartelds *et al.*, 1997).



79 In the current work, the effects of particle flux reduction and porous  
 80 space inaccessibility due to selective flow of different size particles are  
 81 included into the model for deep bed filtration. The terms of advective flux  
 82 reduction and accessibility appear in the population balance equation. An  
 83 analytical solution for the uniform pore size medium shows that deep bed  
 84 filtration does not occur – large particles do not enter the porous media,  
 85 and small particles move without capture.

86 For a small pore size variation medium, an analytical solution found  
 87 shows that only intermediate size particles perform deep bed filtration. In  
 88 this case, the population velocity is particle size-dependent. The averaged  
 89 equations for deep bed filtration of intermediate size particles significantly  
 90 differ from the classical deep bed filtration model.

91 In Section 2, the classical deep bed filtration equations are presented. Its  
 92 stochastic generalization accounting for pore and particle size distributions  
 93 and for flux reduction with pore accessibility is derived in Section 3. The  
 94 initial-boundary value problem for suspension injection has a Goursat type;  
 95 it allows obtaining the exact formulae for captured-particle and pore popu-  
 96 lations at the inlet cross-section without solving the initial-boundary value  
 97 problem (Section 4). Section 5 contains analytical solution for a single pore  
 98 size medium. Exact analytical solution and averaged equations for deep  
 99 bed filtration in a media with small pore size variation are also derived in  
 100 Section 6.

## 101 2. Classical Deep Bed Filtration Model

102 The deep bed filtration system consists of equations for the particle mass  
 103 balance, for the particle capture kinetics and of Darcy's law (Iwasaki, 1937;  
 104 Herzig *et al.*, 1970)

$$\begin{aligned}
 105 \quad & \frac{\partial c(X, T)}{\partial T} + \frac{\partial c(X, T)}{\partial X} = -\frac{1}{\phi} \frac{\partial \sigma(X, T)}{\partial T}, \\
 106 \quad & \frac{\partial \sigma(X, T)}{\partial T} = \lambda(\sigma) \phi c(X, T), \\
 107 \quad & U = -\frac{k_0 k(\sigma)}{\mu L} \frac{\partial p}{\partial X},
 \end{aligned} \tag{1}$$

108 where  $\lambda(\sigma) = \lambda'(\sigma)L$  is the dimensionless filtration coefficient that is equal  
 109 to probability that a particle will be captured during flow through a  
 110 specimen;  $X$  and  $T$  are dimensionless coordinate and time;  $c(X, T)$  is the  
 111 suspended particle concentration that is equal to the number of suspended  
 112 particles per unit of pore space volume;  $\sigma(X, T)$  is the deposited particle  
 113 concentration that is equal to the number of retained particles per unit of



114 porous rock volume. The formation damage function  $k(\sigma)$  shows how per-  
115 meability declines due to particle deposition.

116 The velocity  $U$  is independent of  $X$  due to suspension incompressibility.  
117 Therefore, the third equation (1) separates from the first and second equa-  
118 tions that can be solved independently. The first and second equation (1)  
119 form the kinematics model for transport and capture of particles, the third  
120 equation is a dynamical model that predicts pressure gradient increase due  
121 to permeability decline with the particle retention.

122 In the case of constant filtration coefficient, the particle penetration  
123 depth equals  $1/\lambda$ .

124 In the case of size exclusion capture, the larger are the particles and the  
125 smaller are the pores, the higher is the capture rate. Nevertheless, the phe-  
126 nomenological model (1) does not account for particle and pore size distri-  
127 butions.

128 In the current work, the emphasis is on the size exclusion mechanism of  
129 particle capture in the model accounting for particle and pore size distribu-  
130 tions.

131 It is worth mentioning that particles move with the carrier water veloc-  
132 ity, according to the continuity equation (1). Analytical solution for one-  
133 dimensional deep bed filtration contains the suspended concentration shock  
134 that moves with the carrier water velocity, the particles appear at the core  
135 outlet after one pore volume injected and the suspended and captured con-  
136 centrations are equal to zero ahead of this shock (Herzig *et al.*, 1970).

### 137 3. Governing Equations

138 In this section we derive the population balance equations for flow of water  
139 with suspended particles in porous media. In the derivations of the kinetic  
140 equations, we will proceed from an assumption similar to the Boltzmann's  
141 assumption about "molecular chaos" (Landau and Lifshitz, 1986). Some  
142 particles are captured by the rock from the suspension by size exclusion  
143 mechanism, i.e. if a large particle arrives to a small pore,  $r_p < r_s$ , it is cap-  
144 tured and plugs the pore; otherwise, a small particle  $r_p > r_s$  passes the pore  
145 without being captured (Figure 1). It is also assumed that each particle can  
146 plug only one pore, and vice versa.

147 The geometric model structure of the pore space is as follows:

- 148 • locally the porous space is a bundle of parallel capillary;
- 149 • the flux through each pore is proportional to the fourth power of its  
150 radius;
- 151 • the complete mixing takes place at the length scale  $l$ , i.e. there is a non-  
152 zero probability for a particle moving through any pore at the point  $x$   
153 to get into any pore at the point  $x + l$ .



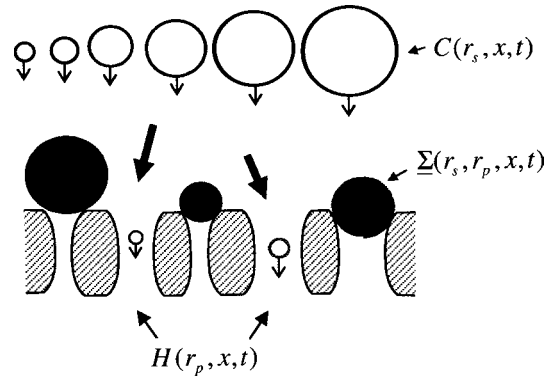


Figure 1. Schema of the large particle entrapment by small pores.

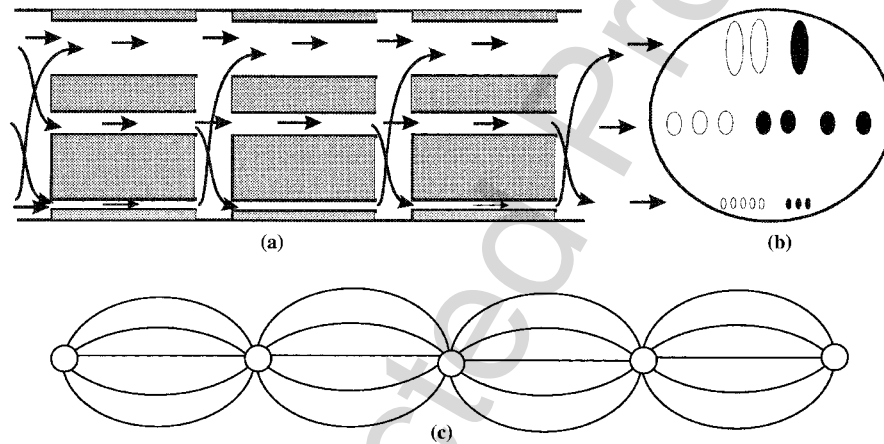


Figure 2. Separation of particle flow and capture by inserting the mixing chambers (sieves) into a capillary bundle porous media: (a) particle trajectories in capillaries and chambers, (b) frontal cross section, (c) schema for links between pores in sequential capillary bundle sections.

154 The example of the porous medium under consideration is shown in  
 155 Figure 2(a)–(c) – it is a bundle of parallel capillary alternated by mix-  
 156 ing chambers. The complete mixing of different size particles occurs in the  
 157 chambers. The particle transport and capture occurring simultaneously in  
 158 natural rocks, are separated in the proposed model. The particles move  
 159 in the sections of a bundle of parallel capillary without being captured  
 160 (Figure 2a). The capture occurs at the thin pore inlet, where large parti-  
 161 cles arrive. So, an inlet cross-section of each parallel capillary section acts  
 162 as a sieve, i.e. large particles do not enter thin pores and are captured at  
 163 chamber outlets.

164 It is assumed that the chamber volume is negligible if compared with the  
 165 capillary (pore) volume.



166 In order to describe the pore size exclusion mechanism, one should  
 167 introduce distributions of suspended particles, captured particles and pores  
 168 over radius

$$169 \int_0^{\infty} f_s(r_s, x, t) dr_s = 1, \quad \int_0^{\infty} f_T(r_s, x, t) dr_s = 1, \quad \int_0^{\infty} f_p(r_p, x, t) dr_p = 1. \quad (2)$$

170 The product  $f_s(r_s, x, t) dr_s$  is the fraction of particles with radii between  
 171  $r_s$  and  $r_s + dr_s$ . The concentration  $C(r_s, x, t) dr_s$  of suspended particles with  
 172 radii between  $r_s$  and  $r_s + dr_s$  is defined as the number of particles with radii  
 173 between  $r_s$  and  $r_s + dr_s$  per unit of pore volume

$$174 C(r_s, x, t) dr_s = c(x, t) f_s(r_s, x, t) dr_s. \quad (3)$$

175 Strictly speaking,  $C(r_s, x, t) dr_s$  is a concentration, and  $C(r_s, x, t)$  is a  
 176 “concentration density”, or “concentration distribution”.

177 The concentration  $c(x, t)$  is the total number of particles per unit of  
 178 pore volume.

179 From Equations (2) and (3) follows that the total particle concentration  
 180 is

$$181 \int_0^{\infty} C(r_s, x, t) dr_s = c(x, t). \quad (4)$$

182 Let us introduce the fraction of particles with radii between  $r_s$  and  
 183  $r_s + dr_s$  have been captured by pores with radii between  $r_p$  and  $r_p + dr_p$ :  
 184  $\underline{f}_T(r_s, r_p, x, t) dr_s dr_p$ . The particle concentration with radius  $r_s$  that have  
 185 been captured by pores with radius  $r_p$  is called  $\underline{\Sigma}(r_s, r_p, x, t)$  (Figure 1):

$$186 \underline{\Sigma}(r_s, r_p, x, t) dr_p dr_s = \sigma(x, t) \underline{f}_T(r_s, r_p, x, t) dr_p dr_s. \quad (5)$$

187 The product  $\underline{\Sigma}(r_s, r_p, x, t) dr_s dr_p$  is equal to the number of particles with  
 188 radii between  $r_s$  and  $r_s + dr_s$  which have been captured by pores with radii  
 189 between  $r_p$ , and  $r_p + dr_p$  per unit of the rock volume.

190 The total retained concentration  $\sigma(x, t)$  is equal to the number of par-  
 191 ticles captured in a unitary volume of a porous medium.

192 The size exclusion capture mechanism assumes that the “ $r_s$ ” particle is  
 193 captured by the “ $r_p$ ” pore if  $r_s > r_p$ . Therefore,  $\underline{\Sigma}(r_s, r_p, x, t) = 0$  for  $r_s < r_p$ ,  
 194 and the fraction of captured particles with radii between  $r_s$  and  $r_s + dr_s$  is

$$195 f_T(r_s, x, t) dr_s = \left[ \int_0^{r_s} \underline{f}_T(r_s, r_p, x, t) dr_p \right] dr_s. \quad (6)$$



196 Integrating (5) in  $r_p$  and accounting for (6), we obtain the concentration  
 197 of captured particles with radius in the interval  $[r_s, r_s + dr_s]$ :

$$198 \quad \left[ \int_0^{r_s} \underline{\Sigma}(r_s, r_p, x, t) dr_p \right] dr_s = \Sigma(r_s, x, t) dr_s. \quad (7)$$

199 From (5)–(7) follows that

$$200 \quad \Sigma(r_s, x, t) dr_s = \sigma(x, t) f_T(r_s, x, t) dr_s. \quad (8)$$

201 Integration of (7) in  $r_s$  from zero to infinity results in the total captured  
 202 particle concentration:

$$203 \quad \int_0^{\infty} \Sigma(r_s, x, t) dr_s = \sigma(x, t). \quad (9)$$

204 The vacant pore concentration  $H(r_p, x, t) dr_p$  with radius in the interval  
 205  $[r_p, r_p + dr_p]$  is defined as

$$206 \quad H(r_p, x, t) dr_p = h(x, t) f_p(r_p, x, t) dr_p, \quad (10)$$

207 where the total vacant pore concentration is

$$208 \quad \int_0^{\infty} H(r_p, x, t) dr_p = h(x, t). \quad (11)$$

209 It is assumed that a captured particle plugs one pore only, and vice  
 210 versa. Besides, the size exclusion mechanism assumes that an  $r_s$ -particle can  
 211 be captured by an  $r_p$ -pore if  $r_s > r_p$ , so  $\underline{\Sigma}(r_s, r_p, x, t) = 0$  for  $r_s < r_p$ . There-  
 212 fore, the variation on the total number of pores with radii in the interval  
 213  $[r_p, r_p + dr_p]$  is equal to the total number of particles captured in pores with  
 214 size in the interval  $[r_p, r_p + dr_p]$ :

$$215 \quad H(r_p, x, t) dr_p = H(r_p, x, 0) dr_p - \left[ \int_{r_p}^{\infty} \underline{\Sigma}(r_s, r_p, x, t) dr_s \right] dr_p. \quad (12)$$

216 Differentiation of (12) with respect to  $t$  results in

$$217 \quad \frac{\partial H(r_p, x, t)}{\partial t} = - \int_{r_p}^{\infty} \frac{\partial \underline{\Sigma}(r_s, r_p, x, t)}{\partial t} dr_s. \quad (13)$$

218 Equation (13) means that plugging of a pore is caused by the capture  
 219 of whatever larger particle.





220 Let us derive the population balance for suspended and captured parti-  
221 cles.

222 A particle with radius  $r_s$  passes through the pore with radius  $r_p$  only if  
223 the particle radius is smaller than the pore radius,  $r_s < r_p$ . Therefore, small  
224 pores ( $r_p < r_s$ ) are inaccessible for large particles. Particles flow in larger  
225 pores only, i.e. in an accessible pore volume. Assuming that locally the pore  
226 space is a bundle of parallel capillary, we introduce the accessibility factor  
227  $\gamma$  for particles with radius  $r_s$  as a fraction of pore volume with capillary  
228 radii larger than  $r_s$ :

$$229 \quad \gamma(r_s, x, t) = \frac{\int_{r_p}^{\infty} r_p^2 H(r_p, x, t) dr_p}{\int_0^{\infty} r_p^2 H(r_p, x, t) dr_p}. \quad (14)$$

230 Consequently, particles with radius  $r_s$  move in the  $\gamma(r_s, x, t)$ -th fraction  
231 of pore volume.

232 Let us define the flux  $J(r_s, r_p, x, t) dr_s / dr_p$  of particles with specific radius  
233  $r_s$  via pores with a specific radius  $r_p$  and also the total flux  $J(r_s, x, t) dr_s$  of  
234 particles with radii in the interval  $[r_s, r_s + dr_s]$ . From the assumption that  
235 locally the pore space is a bundle of parallel capillary, we obtain:

$$236 \quad J(r_s, x, t) dr_s = \left[ \int_{r_s}^{\infty} \underline{J}(r_s, r_p, x, t) dr_p \right] dr_s. \quad (15)$$

237 The flux of particles with radius  $r_s$  via pores with smaller radius ( $r_p < r_s$ )  
238 equals zero. Nevertheless, water flows via pores of all sizes including thin  
239 pores. Therefore, the water flux carrying  $r_s$ -particles is lower than the over-  
240 all water flux in the porous medium.

241 We assume that the flux via the pore  $r_p$  is proportional to the fourth  
242 power of the capillary radius  $r_p^4$  (Hagen–Poiseuille formula, see Landau and  
243 Lifshitz, 1987). Consequently, the fraction of the flux via pores with radii  
244 varying from  $r_p$  to  $r_p + dr_p$  is

$$245 \quad F(r_p, x, t) dr_p = \frac{H(r_p, x, t) r_p^4 dr_p}{\int_0^{\infty} H(r_p, x, t) r_p^4 dr_p}. \quad (16)$$

246 The flux of particles with specific radius  $r_s$  via pores with specific radius  
247  $r_p$  equals the total flux of particles with radius  $r_s$  times fraction of the total  
248 flux via the pores with radius  $r_p$  only:

$$249 \quad \underline{J}(r_s, r_p, x, t) dr_s dr_p = UC(r_s, x, t) \frac{H(r_p, x, t) r_p^4 dr_p}{\int_0^{\infty} H(r_p, x, t) r_p^4 dr_p} dr_s. \quad (17)$$



250 The above explanation of (17) would become more rigorous by substi-  
 251 tuting the terms “specific radius”  $r_s$  and  $r_p$  by the terms “in the intervals”  
 252  $[r_s, r_s + dr_s]$  and  $[r_p, r_p + dr_p]$ , respectively.

253 The total flux  $J(r_s, x, t)dr_s$  of particles with radii in the interval  $[r_s, r_s +$   
 254  $dr_s]$  accounts for transport via all pores with radius larger than  $r_s$ :

$$255 \quad J(r_s, x, t)dr_s = UC(r_s, x, t) \frac{\int_{r_s}^{\infty} H(r_p, x, t)r_p^4 dr_p}{\int_0^{\infty} H(r_p, x, t)r_p^4 dr_p} dr_s. \quad (18)$$

256 Introducing the fraction of the total flux that carries particles with  
 257 radius  $r_s$

$$258 \quad \alpha(r_s, x, t) = \frac{\int_{r_s}^{\infty} r_p^4 H(r_p, x, t) dr_p}{\int_0^{\infty} r_p^4 H(r_p, x, t) dr_p} \quad (19)$$

259 from (18) and (19), we obtain the following formula for the flux of particles  
 260 with radii varying from  $r_s$  to  $r_s + dr_s$ :

$$261 \quad J(r_s, x, t)dr_s = U\alpha(r_s, x, t)C(r_s, x, t) dr_s \quad (20)$$

262 From now on,  $\alpha$  will be called the flux reduction factor.

263 Formulae for the flux reduction and accessibility factors ((14) and (19))  
 264 can be derived for regular pore networks using effective medium or perco-  
 265 lation theories (Sharma and Yortsos, 1987b,c; Seljakov and Kadet, 1996).  
 266 From either theory will follow two threshold values for the flux reduction  
 267 factor corresponding to existence of infinite clusters for small and for large  
 268 particles.

269 In the case of low concentrated suspensions, the pore space fraction  
 270 occupied by retained particles is negligibly small if compared with the over-  
 271 all pore space. Therefore, the porosity is assumed to be constant.

272 From now on, we consider concentration densities instead of concentra-  
 273 tions, so the multipliers  $dr_s$  and  $dr_p$  in both sides of equations are dropped.  
 274 In this case, the equation for particle number balance for  $r_s$ -population  
 275 accounting for retention is

$$276 \quad \phi \frac{\partial[\gamma(r_s, x, t)C(r_s, x, t)]}{\partial t} + \frac{\partial J(r_s, x, t)}{\partial x} = -\frac{\partial \Sigma(r_s, x, t)}{\partial t}. \quad (21)$$

277 Substitution of (20) into (21) results in the following form of the  
 278 population balance equation:

$$279 \quad \phi \frac{\partial[\gamma(r_s, x, t)C(r_s, x, t)]}{\partial t} + \frac{\partial[U\alpha(r_s, x, t)C(r_s, x, t)]}{\partial x} = -\frac{\partial \Sigma(r_s, x, t)}{\partial t}. \quad (22)$$

280 In order to obtain a closed system of governing equations, let us derive  
 281 equations for particle capture and pore plugging rates. The probability  $P$



282 of a particle with radius from the interval  $[r_s, r_s + dr_s]$  to meet a pore with  
 283 radius from the interval  $[r_p, r_p + dr_p]$  is proportional to the product between  
 284 the number of particles with radius from the interval  $[r_s, r_s + dr_s]$  and the  
 285 flux fraction that passes via the pores with radius from the interval  $[r_p, r_p +$   
 286  $dr_p]$  (Herzig *et al.*, 1970):

$$287 \quad P \propto UC(r_s, x, t) dr_s \frac{r_p^4 H(r_p, x, t) dr_p}{\int_0^\infty r_p^4 H(r_p, x, t) dr_p}. \quad (23)$$

288 The number of particles with size in the interval  $[r_s, r_s + dr_s]$  captured  
 289 in pores with radius in the interval  $[r_p, r_p + dr_p]$  per unit of time is called  
 290 the particle-capture rate. This rate is proportional to the probability  $P$ ,  
 291 (23), and the proportionality co-efficient is called the filtration co-efficient  
 292  $-\lambda'(r_s, r_p)$ :

$$293 \quad \frac{\partial \Sigma(r_s, r_p, x, t)}{\partial t} = \lambda'(r_s, r_p) UC(r_s, x, t) \frac{r_p^4 H(r_p, x, t)}{\int_0^\infty r_p^4 H(r_p, x, t) dr_p}. \quad (24)$$

294 Here, as in the majority of following formulae, we omitted  $dr_s/dr_p$  in both  
 295 sides of (24). It means that we will work with concentrations density ( $C$ ,  $\Sigma$   
 296 and  $H$ ) instead of concentrations ( $Cdr_s$ ,  $\Sigma dr_s$ , and  $H-dr_p$ ).

297 The filtration coefficient is equal to zero for the absence of capture:

$$298 \quad \lambda'(r_s, r_p) = 0: \quad r_p > r_s. \quad (25)$$

299 Integration of both sides of (24) over  $r_p$  from zero to infinity and  
 300 accounting for (25), results in the expression for the total capture rate of  
 301 particles with radius  $r_s$ :

$$302 \quad \frac{\partial \Sigma(r_s, x, t)}{\partial t} = \frac{UC(r_s, x, t)}{\int_0^\infty r_p^4 H(r_p, x, t) dr_p} \int_0^{r_s} \lambda'(r_s, r_p) H(r_p, x, t) dr_p. \quad (26)$$

303 Substituting the capture rate (24) into (13), we obtain the equation for  
 304 pore plugging kinetics

$$305 \quad \frac{\partial H(r_p, x, t)}{\partial t} = \frac{UH(r_p, x, t)r_p^4}{\int_0^\infty H(r_p, x, t)r_p^4 dr_p} \int_{r_p}^\infty \lambda'(r_s, r_p) C(r_s, x, t) dr_s. \quad (27)$$

306 It is assumed that the aqueous suspension is incompressible, the total  
 307 flux conserves,  $U = U(t)$ , and term  $U$  can be taken out of  $x$ -derivative in  
 308 Equation (22).



309 Equations (22), (26) and (27) form a closed system for three unknowns  
 310  $C(r_s, x, t)$ ,  $\Sigma(r_s, x, t)$  and  $H(r_p, x, t)$ :

$$\begin{aligned}
 311 \quad & \phi \frac{\partial[\gamma(r_s, x, t)C(r_s, x, t)]}{\partial t} + U \frac{\partial[\alpha(r_s, x, t)C(r_s, x, t)]}{\partial x} = - \frac{\partial \Sigma(r_s, x, t)}{\partial t}, \\
 312 \quad & \frac{\partial \Sigma(r_s, x, t)}{\partial t} = UC(r_s, x, t) \frac{\int_0^{r_s} \lambda'(r_s, r_p) r_p^4 H(r_p, x, t) dr_p}{\int_0^\infty r_p^4 H(r_p, x, t) dr_p}, \quad (28) \\
 313 \quad & \frac{\partial H(r_p, x, t)}{\partial t} = -U \frac{r_p^4 H(r_p, x, t)}{\int_0^\infty r_p^4 H(r_p, x, t) dr_p} \int_{r_p}^\infty \lambda'(r_s, r_p) C(r_s, x, t) dr_s.
 \end{aligned}$$

314 Introduction of dimensionless variables

$$315 \quad x = \frac{x}{L}, \quad T = \frac{UT}{L\phi}, \quad \lambda = \lambda' L, \quad (29)$$

316 transforms the system (28) to the form:

$$\begin{aligned}
 & \frac{\partial[\gamma(r_s, X, T)C(r_s, X, T)]}{\partial T} + U \frac{\partial[\alpha(r_s, X, T)C(r_s, X, T)]}{\partial X} \\
 & = - \frac{1}{\phi} \frac{\partial \Sigma(r_s, X, T)}{\partial T}, \\
 & \frac{\partial \Sigma(r_s, X, T)}{\partial T} = \phi C(r_s, X, T) \frac{\int_0^{r_s} \lambda(r_s, r_p) r_p^4 H(r_p, X, T) dr_p}{\int_0^\infty r_p^4 H(r_p, X, T) dr_p}, \quad (30) \\
 317 \quad & \frac{\partial H(r_p, X, T)}{\partial T} = -\phi \frac{r_p^4 H(r_p, X, T)}{\int_0^\infty r_p^4 H(r_p, X, T) dr_p} \int_{r_p}^\infty \lambda(r_s, r_p) C(r_s, X, T) dr_s.
 \end{aligned}$$

318 Boundary condition at the core inlet corresponds to injection of water  
 319 with a given particle size distribution  $C^{(0)}(r_s, T)$ . The injected  $r_s$ -particle  
 320 flux is equal to  $C^{(0)}(r_s, T)U$ . The inlet core/reservoir cross-section acts as  
 321 a sieve. The injected  $r_s$ -particles are carried into the porous medium by a  
 322 fraction of the water flux via accessible pores –  $\alpha^{(0)}(r_s, T)U$  (Figure 2(b)).  
 323 The injected  $r_s$ -particles carried by water flux via inaccessible pores  $[1 -$   
 324  $\alpha^{(0)}(r_s, T)]U$  are deposited at the outer surface of the inlet and form the  
 325 external filter cake from the very beginning of injection. For particles larger  
 326 than any pore, there is no accessible pores and flux reduction factor is zero,  
 327  $\alpha^{(0)}(r_s, T) = 0$ . So, all these particles are retained at the inlet cross-section,  
 328 contributing to external filter cake growth. On the other hand, for particles  
 329 smaller than the smallest pore,  $\alpha^{(0)}(r_s, T) = 1$ . So, all these particles enter  
 330 porous medium without being captured.

331 The density of the  $r_s$ -particle flux entering porous medium (in situ  
 332  $r_s$ -particle flux) is equal to  $C^{(0)}(r_s, T)\alpha^{(0)}(r_s, T)U$ ; and the fraction captured



333 at the inlet cross-section is equal to  $C^{(0)}(r_s, T)[1 - \alpha^{(0)}(r_s, T)]U$ . Therefore,  
 334 the  $r_s$ -particle concentration is continuous at  $X = 0$ .

335 We also assume that the retained at the outer surface of the inlet large  
 336 particles do not restrict access of newly arriving particles to the core inlet  
 337 before the transition time (Khatib, 1994; Pang and Sharma, 1994). The  
 338 external cake does not form a solid matrix before the transition time and  
 339 cannot capture the particles from the injected suspension.

340 Initial condition corresponds to the absence of either suspended or cap-  
 341 tured particles in porous media before the flow. Finally,

$$X = 0: C(r_s, 0, T) = C^{(0)}(r_s, T), \quad (31)$$

$$342 \quad T = 0: C(r_s, X, 0) = 0, \quad \Sigma(r_s, X, 0) = 0, \quad H(r_p, X, 0) = H_0(r_p, X).$$

343 Integration of (13) in  $r_p$ , from zero to infinity results in a conservation  
 344 law for pore number

$$345 \quad \frac{\partial h}{\partial T} = -\frac{\partial \sigma}{\partial T}, \quad (32)$$

346 which leads to

$$347 \quad h(X, T) = h_0(X) - \sigma(X, T). \quad (33)$$

348 Equation (33) shows that one particle can plug only one pore and vice  
 349 versa.

#### 350 4. Particle and Pore Populations at the Inlet Cross-Section

351 Second and third equations of system (30) do not contain  $X$ -derivative, so  
 352 it is not necessary to set the corresponding species concentrations at the  
 353 inlet boundary  $X = 0$  (The so-called Goursat problem; Tikhonov and Sa-  
 354 marskii, 1990). It means that one do not fix the injected concentration of  
 355 an immobile specie, i.e. retained particles and vacancies. Nevertheless, these  
 356 values can be calculated using boundary conditions for mobile species and  
 357 the kinetic equations for immobile species (second and third equation of  
 358 system (30)).

359 Let us fix  $X = 0$  in system (30) and substitute the boundary condition  
 360 (31) into second and third equations of system (30). Finally, we obtain the  
 361 system of two ordinary integro-differential equations for captured particle  
 362 and vacant pore concentrations at the plug inlet:

$$363 \quad \begin{aligned} \frac{d\Sigma^{(0)}(r_s, T)}{dT} &= \phi C^{(0)}(r_s, T) \frac{\int_0^{r_s} \lambda(r_s, r_p) r_p^4 H^{(0)}(r_p, T) dr_p}{\int_0^\infty r_p^4 H^{(0)}(r_p, T) dr_p}, \\ \frac{dH^{(0)}(r_p, T)}{dT} &= -\phi \frac{r_p^4 H^{(0)}(r_p, T)}{\int_0^\infty r_p^4 H^{(0)}(r_p, T) dr_p} \int_{r_p}^\infty \lambda(r_s, r_p) C^{(0)}(r_s, T) dr_s, \end{aligned} \quad (34)$$



364 where,

$$365 \quad H^{(0)}(r_p, T) = H(r_p, X = 0, T), \quad \Sigma^{(0)}(r_s, T) = \Sigma(r_s, X = 0, T). \quad (35)$$

366 The second equation (34) is independent of the first equation, and can  
367 be solved separately. Afterwards, the first equation allows calculating the  
368 deposition kinetics.

369 There were no deposited particles and plugged pores at the beginning  
370 of deep bed filtration. It provides the initial conditions for the system of  
371 ordinary integro-differential Equations (34).

$$372 \quad \Sigma^{(0)}(r_p, T = 0) = 0, \quad H^{(0)}(r_p, T = 0) = H_0^{(0)}(r_p). \quad (36)$$

373 The solution of the second ordinary integro-differential Equation (34)  
374 allows calculating the transition time ( $T_{tr}$ ) from the system of deep bed fil-  
375 tration in porous media. The filtration at the inlet cross-section stops at the  
376 moment when the concentration of vacancies  $H^{(0)}(r_p, T)$  forming an infi-  
377 nite cluster decreases up to percolation threshold.

378 The solution  $H^{(0)}(r_p, T)$  results in calculation of the  $r_s$ -particle flux  
379  $C^{(0)}(r_s, T)[1 - \alpha^{(0)}(r_s, T)]U$  forming an external filter cake from the very  
380 beginning of the particle injection. It allows describing the external filter  
381 cake formation before the transition time, when particles still penetrate into  
382 porous medium.

### 383 5. Filtration in a Single Pore Size Medium

384 Consider the injection of suspension with any given particle size distribu-  
385 tion in a porous medium with a single pore radius  $r'_p$ :

$$386 \quad H(r_p, X, T) = h(X, T)\delta(r_p - r'_p). \quad (37)$$

387 Figure 3(a) shows the pore size distribution (Dirac's delta function) at  
388  $T = 0$  and the particle size distribution in the injected suspension at  $X = 0$ .

389 Let us first consider propagation of small particles with  $r_s < r'_p$ . For this  
390 case, formulae (14) and (19) show that  $\alpha = \gamma = 1$ ; i.e. all pores are accessible  
391 for small particles, and there is no flux reduction.

392 Substitution of the pore size distribution (37) into (30) results in the fol-  
393 lowing system for deep bed filtration of small particles:

$$\frac{\partial C(r_s, X, T)}{\partial T} + \frac{\partial C(r_s, X, T)}{\partial X} = 0, \quad (38)$$

$$394 \quad \frac{\partial \Sigma(r_s, X, T)}{\partial T} = 0.$$



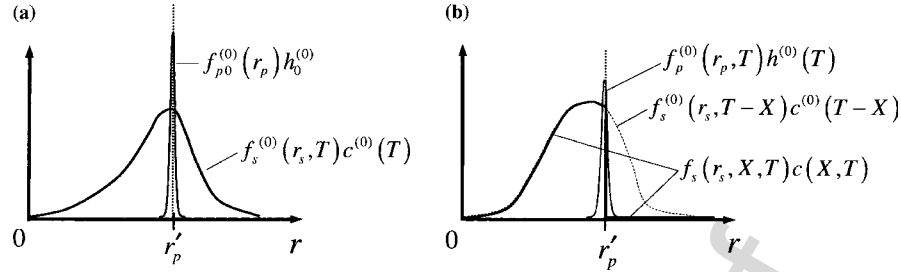


Figure 3. Distributions of suspended particles and pores in a single pore size medium: (a) initial and boundary concentration distributions for pores and suspended particles, respectively; (b) particle distribution for any  $X$  and  $T$  (continuous curve) and at  $X=0$  (dashed curve); pore distribution at the inlet cross-section for  $T > 0$ .

395 The solution of a linear hyperbolic equation (first Equation (38)) subject  
 396 to initial-boundary conditions (31) is a travelling wave:

$$397 \quad C(r_s, X, T) = \begin{cases} C^{(0)}(r_s, T - X), & X < T, \\ 0, & X > T. \end{cases} \quad (39)$$

398 Therefore, small particles are transported with the velocity of carrier  
 399 water without being trapped. There are no suspended particles ahead of  
 400 the injected water front. Particle distribution profile behind the front moves  
 401 with unitary velocity along the porous medium. It repeats the shape of the  
 402 injected concentration  $C^{(0)}(r_s, T)$  with delay that equals  $X$ .

403 We consider the case where there were no trapped particles in porous  
 404 medium before the injection (initial condition (31)). As it follows from the  
 405 second Equation (38), the capture of small particles does not happen. Con-  
 406 sequently, for any  $T \geq 0$

$$407 \quad \Sigma(r_s, X, T) = 0. \quad (40)$$

408 Therefore, no pores will be plugged by small particles.

409 Now consider propagation of large particles ( $r_s > r'_p$ ). In this case, from  
 410 (14) and (19) follows that  $\alpha = \gamma = 0$ .

411 Therefore, none of pores is accessible for large particles, and there is no  
 412 large particle flux.

413 Substitution of (37) into (30) results in the following system:

$$414 \quad 0 = \frac{\partial \Sigma(r_s, X, T)}{\partial T},$$

$$415 \quad \frac{\partial \Sigma(r_s, X, T)}{\partial T} = \phi C(r_s, X, T) \lambda(r_s, r'_p), \quad (41)$$

$$416 \quad \frac{\partial h(X, T)}{\partial T} = -\phi \int_{r'_p}^{\infty} \lambda(r_s, r'_p) C(r_s, X, T) dr_s.$$

417 From initial condition (31) and first Equation (41) follows that

$$418 \quad \Sigma(r_s, X, T) = 0, \quad (42)$$

419 i.e. no large particles are deposited in the reservoir.

420 From first equation (34) we obtain the captured particle concentration  
421 at the core inlet:

$$422 \quad \Sigma^{(0)}(r_s, T) = \lambda(r_s, r'_p) \phi \int_0^T C^{(0)}(r_s, T) dT. \quad (43)$$

423 Therefore, all large particles are captured at the inlet cross-section.

424 It is assumed that there were no suspended particles before the injection  
425 (initial condition (31)). In this case, from first and second equation (41) fol-  
426 lows that:

$$427 \quad C(r_s, X, T) = 0 : X > 0, \quad (44)$$

428 i.e. no large particles ( $r_s > r'_p$ ) enter the reservoir.

429 Substituting (44) into third equation (41) and solving the resulting ordi-  
430 nary differential equation, accounting for initial and boundary conditions  
431 (31), we obtain:

$$432 \quad h(X, T) = h_0(X) : X > 0, \quad (45)$$

433 i.e. the number of vacant pores does not change during the injection.

434 The line 2 in Figure 4 shows that large particles never arrive to the core  
435 outlet. It was also observed in laboratory study (Massei *et al.*, 2002), where  
436 size exclusion was the dominant capture mechanism.

437 Now let us study accumulation of large particles at the core inlet.  
438 Substituting (43) into (9), accounting for (44), results in:

$$439 \quad \sigma^{(0)}(T) = \phi \int_{r'_p}^{\infty} \lambda(r_s, r'_p) \int_0^T C^{(0)}(r_s, \tau) d\tau dr_s. \quad (46)$$

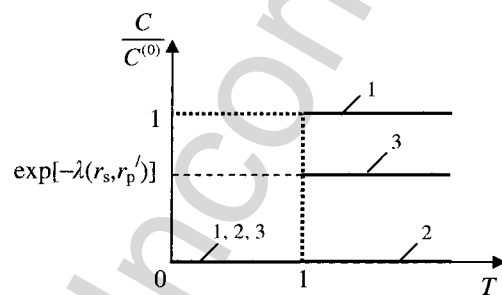


Figure 4. Breakthrough curves for different size particles (at  $X=1$ ): 1 – for particles smaller than  $r'_p$  by the proposed model 2 – for particles larger than  $r'_p$  by the proposed model 3 – for particles larger than  $r'_p$  by the model without considering the flux reduction and accessibility.





440 The equation for vacant pore concentration at the inlet cross-section is  
 441 obtained substituting (46) into (33):

$$442 \quad h^{(0)}(T) = h_0^{(0)} - \sigma^{(0)}(T). \quad (47)$$

443 The relationship (47) reflects the fact that each particle can plug only  
 444 one pore and viceversa.

445 For the case of a single pore size medium (37), the solution of the sys-  
 446 tem (30), subject to the initial and boundary conditions (31), is given by  
 447 formulae (39), (40), (42)–(47).

448 The plot of the solution is given in Figure 3. Initial concentration den-  
 449 sity for pores and concentration density for suspended particles at inlet  
 450 cross-section are shown in Figure 3(a).

451 The dynamics of particle size distributions (PDF) for small and large  
 452 particles is shown in Figure 3(b). Comparison between continuous and dot-  
 453 ted lines shows that the shape of small particle concentration density is  
 454 repeated with delay that is equals to  $X$ , which corresponds to travelling  
 455 wave behaviour, (39). The continuous line in Figure 3b shows that the  
 456 large particle ( $r_s > r'_p$ ) concentration density is equal to zero for any  $X > 0$ .  
 457 Figure 3a and b shows that the total vacancy concentration at the inlet  
 458 cross-section decreases with time, as suggested by formula (47); the pore  
 459 size distribution at  $T > 0$  remains delta function.

460 Figure 4 (line 1) shows concentration density of small particles at the  
 461 core outlet for the case of constant injected concentration. The concen-  
 462 tration equals zero until the injection of one pore volume. After particle  
 463 arrival at the outlet at the moment  $T = 1$ , the concentration at the outlet  
 464 is equal to the injected concentration. The line 2 in Figure 4 shows that  
 465 large particles never arrive to the core outlet.

466 It is important to highlight that, depending on the size, the particles in  
 467 uniform pore size medium either pass or are trapped (see Equations (39)  
 468 and (44)). Therefore, the deep bed filtration, where does exist an average  
 469 penetration length for each size particle, does not happen in case of par-  
 470 ticulate flow in a single-size porous medium. The penetration length is zero  
 471 for large particles, and is infinite for small particles.

472 Let us obtain equations for average concentrations for the case of  
 473 particulate suspension flow in a single pore size medium.

474 Integration of both sides of system (38) in  $r_s$  from zero to  $r'_p$  results in  
 475 the system for average concentration of small particles

$$476 \quad \begin{aligned} \frac{\partial c_1(X, T)}{\partial T} + \frac{\partial c_1(X, T)}{\partial X} &= 0, \\ \frac{\partial \sigma_1(X, T)}{\partial T} &= 0, \end{aligned} \quad (48)$$



477 where

$$c_1(X, T) = \int_0^{r'_p} C(r_s, X, T) dr_s, \quad \sigma_1(X, T) = \int_0^{r'_p} \Sigma(r_s, X, T) dr_s.$$

478

479 The solution of (48), accounting for initial and boundary conditions  
480 (31), is:

$$c_1(X, T) = \begin{cases} c_1^{(0)}(T - X), & X < T, \\ 0, & X > T. \end{cases} \quad (49)$$

481

482 The solution (49) shows that free advection (without particle capture) of  
483 small particles occurs. Thus, deep bed filtration of small particles does not  
484 happen.

485 Integration of both sides of the first and second equation (41) in  $r_s$  from  
486  $r'_p$  to infinity results in the system for average concentration of large parti-  
487 cles  $r_s > r'_p$ :

$$0 = -\frac{1}{\phi} \frac{\partial \sigma_2(X, T)}{\partial T},$$

$$\frac{\partial \sigma_2(X, T)}{\partial T} = \phi \int_{r'_p}^{\infty} \lambda(r_s, r'_p) C(r_s, X, T) dr_s, \quad (50)$$

488

489 where  $\sigma_2$  is the average deposited concentration of large particles.

490 From first equation (50) and initial condition (31) we obtain the solu-  
491 tion for average deposited concentration of large particles:

$$492 \quad \sigma_2(X, T) = 0. \quad (51)$$

493 Substituting first equation (50) into second equation (50) we obtain:

$$\int_{r'_p}^{\infty} \lambda(r_s, r'_p) C(r_s, X, T) dr_s = 0. \quad (52)$$

494

495 Consequently, the average suspended particle concentration is also zero  
496 in the reservoir:

$$\int_{r'_p}^{\infty} C(r_s, X, T) dr_s = c_2(X, T) = 0. \quad (53)$$

497

498 The solutions of (51) and (53) show that all large particles are captured  
499 at the inlet cross-section; there is no transport of large particles through  
500 porous media.



501 In order to evaluate the effect of flux reduction and accessibility on  
 502 particulate suspension flow in porous media, let us ignore the flux reduc-  
 503 tion and accessibility factors in the system of governing equations (30), i.e.  
 504  $\alpha = \gamma = 1$ . In this case, we obtain the population balance model as pre-  
 505 sented by Sharma and Yortsos (1987). Substituting  $\alpha = \gamma = 1$  in the first  
 506 equation (30), results in:

$$507 \quad \frac{\partial C(r_s, X, T)}{\partial T} + \frac{\partial C(r_s, X, T)}{\partial X} = -\frac{1}{\phi} \frac{\partial \Sigma(r_s, X, T)}{\partial T}. \quad (54)$$

508 The second and the third equations of system (30) remain the same. So,  
 509 the system of equations (30) takes the following form:

$$510 \quad \frac{\partial C(r_s, X, T)}{\partial T} + \frac{\partial C(r_s, X, T)}{\partial X} = -\frac{1}{\phi} \frac{\partial \Sigma(r_s, X, T)}{\partial T},$$

$$511 \quad \frac{\partial \Sigma(r_s, X, T)}{\partial T} = \phi C(r_s, X, T) \frac{\int_0^{r_s} \lambda(r_s, r_p) r_p^4 H(r_p, X, T) dr_p}{\int_0^\infty r_p^4 H(r_p, X, T) dr_p}, \quad (55)$$

$$512 \quad \frac{\partial H(r_p, X, T)}{\partial T} = -\phi \frac{r_p^4 H(r_p, X, T)}{\int_0^\infty r_p^4 H(r_p, X, T) dr_p} \int_{r_p}^\infty \lambda(r_s, r_p) C(r_s, X, T) dr_s.$$

513 Let us discuss the case of a single pore size medium. In this case,  
 514  $H(r_p, X, T)$  is defined by Equation (37). The system (55) is reduced to the  
 515 system (38) for small particles with  $r_s < r'_p$ . The solution for this system is  
 516 given in the Equations (39) and (40). The accessibility and flux reduction  
 517 factors are equal unity for small particles, i.e. all pores are accessible, and  
 518 systems (30) and (55) coincide.

519 For large particles with  $r_s > r'_p$ , system (55) takes the following form:

$$520 \quad \frac{\partial C(r_s, X, T)}{\partial T} + \frac{\partial C(r_s, X, T)}{\partial X} = -\frac{1}{\phi} \frac{\partial \Sigma(r_s, X, T)}{\partial T},$$

$$521 \quad \frac{\partial \Sigma(r_s, X, T)}{\partial T} = \lambda(r_s, r'_p) \phi C(r_s, X, T), \quad (56)$$

$$522 \quad \frac{\partial h(X, T)}{\partial T} = -\phi \int_{r'_p}^\infty \lambda(r_s, r'_p) C(r_s, X, T) dr_s.$$

523 Substitution of the second equation (56) into the first one results in one  
 524 equation for suspended particle population:

$$525 \quad \frac{\partial C(r_s, X, T)}{\partial T} + \frac{\partial C(r_s, X, T)}{\partial X} = -\lambda(r_s, r'_p) C(r_s, X, T). \quad (57)$$

526 The solution of the linear hyperbolic Equation (57) with initial and  
 527 boundary conditions (31) for each particle population with particle size



528  $r_s$  is:

$$529 \quad C(r_s, X, T) = \begin{cases} C^{(0)}(r_s, T - X) \exp[-\lambda(r_s, r'_p)X], & X < T, \\ 0, & X > T. \end{cases} \quad (58)$$

530 The solution (58) shows separate deep bed filtration of each popula-  
531 tion of large particles with the particle-size-dependent filtration coefficient  
532  $\lambda(r_s, r'_p)$ .

533 The concentration history at the core outlet according to (58) is shown  
534 in Figure 4 by line 3. Concentration equals zero until the injection of  
535 one pore volume. At the moment  $T = 1$  the concentration front arrives  
536 at the core outlet, and the concentration is constant after the break-  
537 through. The ratio between the injected and effluent concentrations equals  
538  $\exp[-\lambda(r_s, r'_p)]$ , so it is always less than unity, i.e. the produced concentra-  
539 tion density is lower than the injected concentration density.

540 The expression for vacancy concentration is:

$$541 \quad h(X, T) = \begin{cases} h_0(X) - \phi \int_{r'_p}^{\infty} \lambda(r_s, r'_p) \exp[-\lambda(r_s, r'_p)X] \times \\ \quad \times \int_X^T C^{(0)}(r_s, T) dT dr_s, & X < T, \\ h_0(X), & X > T. \end{cases} \quad (59)$$

542 Therefore, ignoring the fact that particles move only via larger pores,  
543 results in a separate deep bed filtration of large particle populations with  
544 different radii in a single pore size medium, while accounting for this effect  
545 results in the absence of deep bed filtration in this porous medium.

## 546 6. Filtration in a Medium with Small Pore Size Variation

547 Let us discuss porous medium with small pore size variation, i.e. pore  
548 radius varies inside the interval  $[r_{p\min}, r_{p\max}]$ , and  $r_{p\max} - r_{p\min} \ll r_{p\min}$   
549 (Figure 5(a)). Pore radius is uniformly distributed inside the interval  
550  $[r_{p\min}, r_{p\max}]$ . Injected particle radius is distributed according to any arbi-  
551 trary probability distribution function, which is independent of time  
552  $f_s^{(0)}(r_s)$ .

### 553 6.1. ANALYTICAL SOLUTION

554 Assuming a uniform pore size distribution, from (10) we obtain:

$$555 \quad H(r_p, x, t) = \begin{cases} 0, & r_p > r_{p\max} \text{ OR } r_p < r_{p\min}, \\ \frac{h(x, t)}{r_{p\max} - r_{p\min}}, & r_{p\min} < r_p < r_{p\max}. \end{cases} \quad (60)$$



556 Substitution of (60) into (14) and (19) allows obtaining expressions  
 557 for flux reduction and accessibility factors for intermediate size particles  
 558 ( $r_{p\min} < r_s < r_{p\max}$ ):

$$559 \quad \alpha(r_s) = \frac{r_{p\max}^5 - r_s^5}{r_{p\max}^5 - r_{p\min}^5}, \quad (61)$$

$$561 \quad \gamma(r_s) = \frac{r_{p\max}^3 - r_s^3}{r_{p\max}^3 - r_{p\min}^3}, \quad (62)$$

562 i.e. the fractions  $\alpha$  and  $\gamma$  become just  $r_s$ -dependent. Consequently, system  
 563 (30) takes the form:

$$564 \quad \gamma(r_s) \frac{\partial C(r_s, X, T)}{\partial T} + \alpha(r_s) \frac{\partial C(r_s, X, T)}{\partial X} = -\frac{1}{\phi} \frac{\partial \Sigma(r_s, X, T)}{\partial T},$$

$$565 \quad \frac{\partial \Sigma(r_s, X, T)}{\partial T} = \phi \eta(r_s) C(r_s, X, T), \quad (63)$$

$$566 \quad \frac{\partial H(r_p, X, T)}{\partial T} = -\phi \frac{r_p^4 H(r_p, X, T)}{\int_0^\infty r_p^4 H(r_p, X, T) dr_p} \int_{r_p}^\infty \lambda(r_s, r_p) C(r_s, X, T) dr_s,$$

567 where,

$$568 \quad \eta(r_s) = \begin{cases} 0, & r_s < r_{p\min}, \\ \frac{\int_{r_{p\min}}^{r_s} \lambda(r_s, r_p) r_p^4 dr_p}{\int_{r_{p\min}}^{r_{p\max}} r_p^4 dr_p}, & r_{p\min} < r_s < r_{p\max}, \\ \frac{\int_{r_{p\min}}^{r_{p\max}} \lambda(r_s, r_p) r_p^4 dr_p}{\int_{r_{p\min}}^{r_{p\max}} r_p^4 dr_p}, & r_s \geq r_{p\max}. \end{cases} \quad (64)$$

569 For small ( $r_s < r_{p\min}$ ) and large ( $r_s > r_{p\max}$ ) particles, system (63) coincide  
 570 with systems (38) and (41), respectively. Therefore, the solution for small parti-  
 571 cles is given by formulae (39), (40) and the solution for large particles is given  
 572 by (42)–(47). Small particles are transported through porous medium without  
 573 being captured and all large particles are captured at the inlet cross section.  
 574 Consequently, small and large particles do not perform deep bed filtration.

575 Figure 5(b) shows the injected particle concentration (dotted line) and  
 576 the concentration density of suspended particles behind the front for  $T > 0$ .  
 577 Both concentrations coincide for small particles ( $r_s < r_{p\min}$ ).

578 On the other hand, intermediate size particles ( $r_{p\min} < r_s < r_{p\max}$ ) per-  
 579 form deep bed filtration, i.e., a fraction of each particle population is cap-  
 580 tured during the transport of particles through porous media.

581 Let us discuss deep bed filtration of intermediate size particles.

582 Substitution of second Equation (63) into the first one results in:

$$583 \quad \gamma(r_s) \frac{\partial C(r_s, X, T)}{\partial T} + \alpha(r_s) \frac{\partial C(r_s, X, T)}{\partial X} = -\eta(r_s) C(r_s, X, T). \quad (65)$$



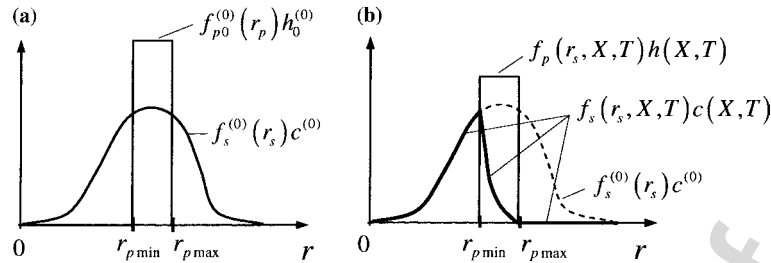


Figure 5. Distributions for suspended particles and pores in a medium with small pore size variation: (a) initial and boundary distributions for pores and suspended particles, respectively; (b) suspended particle distributions behind the concentration front for  $T > 0$  (solid curve) and in the injected suspension (dashed curve), and vacancy distribution.

584 The solution of linear hyperbolic Equation (65) is obtained by method  
585 of characteristics:

$$C(r_s, X, T) = \begin{cases} C^{(0)}(r_s) \exp\left[-\frac{\eta(r_s)}{\alpha(r_s)} X\right], & X < \frac{\alpha(r_s)}{\gamma(r_s)} T \\ 0, & X > \frac{\alpha(r_s)}{\gamma(r_s)} T \end{cases}. \quad (66)$$

586

587 The concentration distribution of particles with a specific size is steady  
588 state behind the concentration front, and is zero ahead of the front.

589 The total suspended concentration  $c(X, T)$  can be calculated from (66)  
590 using formula (4).

591 Substituting (66) into second equation (30) and solving the resulting  
592 equation, we obtain expression for the deposited particles population:

$$\Sigma(r_s, X, T) = \begin{cases} \eta(r_s)\phi\left[T - \frac{\gamma(r_s)}{\alpha(r_s)} X\right] C^{(0)}(r_s) \exp\left[-\frac{\eta(r_s)}{\alpha(r_s)} X\right], & X < \frac{\alpha(r_s)}{\gamma(r_s)} T \\ 0, & X > \frac{\alpha(r_s)}{\gamma(r_s)} T \end{cases}, \quad (67)$$

593

594 where  $\alpha(r_s)$  and  $\gamma(r_s)$  are given by (61) and (62), respectively.

595 The characteristic velocity in (65) is particle-size dependent:

$$\frac{dX}{dT} = \frac{\alpha(r_s)}{\gamma(r_s)}. \quad (68)$$

596

597 In the case where the filtration coefficient is independent of pore radius,  
598  $\lambda = \lambda(r_s)$ , from (64) we obtain:

$$\eta(r_s) = \lambda(r_s)[1 - \alpha(r_s)]. \quad (69)$$

599

600 In the case of a bundle of parallel capillary, the dependency of the par-  
601 ticle velocity on  $r_s$  is obtained by substitution of (61) and (62) into (68).

602 Figure 6 shows that the larger is the particle, the larger is its velocity. The



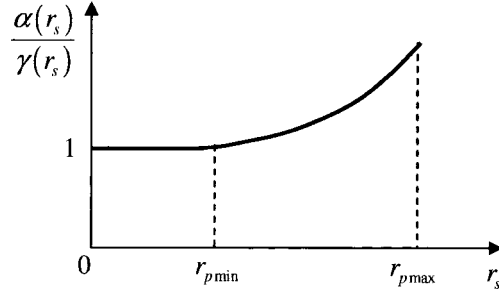


Figure 6. Particle velocity versus its radius.

603 large particles are the first to appear at the core outlet. This phenomenon  
 604 was observed for deep bed filtration with size exclusion of particles (Massei  
 605 *et al.*, 2002) and for flow of polymer solution in a porous media (Bartelds  
 606 *et al.*, 1997).

607 As it follows from (61), (62) and (66), for particles with  $r_s = r_{p\min}$  ( $\alpha = 1$   
 608 and  $\gamma = 1$ ), there is no velocity enhancement, particles move with the veloc-  
 609 ity of carrier water.

610 The larger is the particle the higher is the decrement in the exponent of  
 611 the solution (66). Consequently, the larger is the particle the more intensive  
 612 is the particle capture rate.

613 When  $r_s$  tends to  $r_{p\max}$ , the denominator in the exponent in (66) tends  
 614 to zero, and the concentration tends to zero. The concentration density of  
 615 intermediate size particles  $C(r_s, X, T)$  in Figure 5(b) decreases from the ini-  
 616 tial value  $C^{(0)}(r_s = r_{p\min})$  at  $r_s = r_{p\min}$  to zero for  $r_s = r_{p\max}$ .

617 Substituting (60) into first equation (34) we obtain deposited concentra-  
 618 tions at the core Inlet:

$$619 \quad \Sigma^{(0)}(r_s, T) = \eta(r_s)\phi C^{(0)}(r_s)T. \quad (70)$$

620 Here  $\eta = 0$  for particles with radii smaller than  $r_{p\min}$  (see (64)), i.e., small  
 621 particles ( $r_s < r_{p\min}$ ) pass the core inlet without being captured. Particles  
 622 with radii larger than  $r_{p\max}$  do not enter the rock and are deposited at  
 623 the inlet cross section. From (9) follows the formula for the total deposited  
 624 concentration at the core inlet:

$$625 \quad \sigma^{(0)}(T) = \int_{r_{p\min}}^{\infty} \Sigma^{(0)}(r_s, T) dr_s. \quad (71)$$

626 Formula (33), accounting for (70) and (71), allows calculation of the  
 627 total vacancy concentration at the rock inlet.

628 Figure 7 shows concentration profiles for different intermediate size  
 629 particles. The suspended concentration wave front moves with velocity  
 630  $\alpha(r_s)/\gamma(r_s)$ .



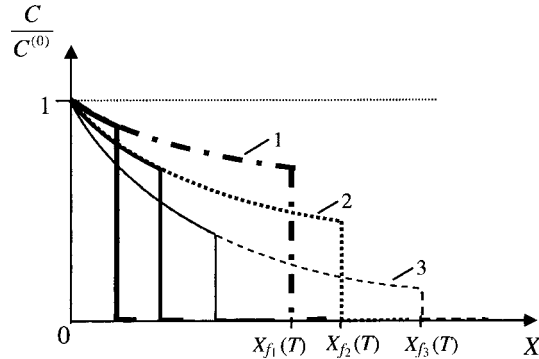


Figure 7. Concentration distribution profiles for intermediate size particles during filtration in a small pore size variation medium. Lines 1, 2 and 3 correspond to different particle populations ( $r_{s1} < r_{s2} < r_{s3}$ ).

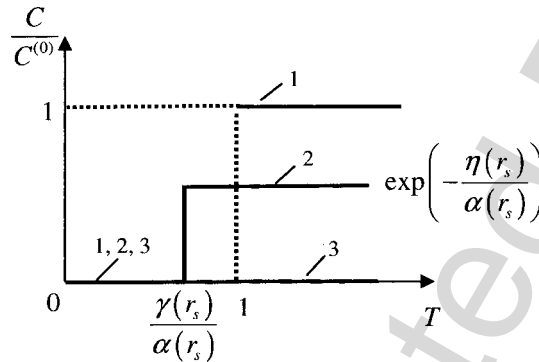


Figure 8. Particle concentration distribution histories at the core outlet, Line (1) corresponds to concentration of particles smaller than  $r_{pmin}$ ; line (2) is related to concentration of an intermediate size particles ( $r_{pmin} < r_s < r_{pmax}$ ); line (3) corresponds to concentration of particles larger than  $r_{pmax}$ .

631 The steady state profile behind the front for each particle population  
 632  $C(r_s, X)$  is given by first formula (66). Figure 7 shows that for each size  
 633 particles, the profile at the moment  $T_1$  and the section of the profile at the  
 634 moment  $T_2$  from zero to  $\alpha(r_s)/\gamma(r_s)T_2$  coincide.

635 The larger are the particles the higher is the decrement  $\eta(r_s)/\alpha(r_s)$   
 636 of exponent in (66), so small particles have higher relative concentration  
 637  $(C(r_s, X, T)/C^{(0)}(r_s))$  and their concentration profile moves slowly.

638 Figure 8 shows different particle size concentration history at the core  
 639 outlet ( $X = 1$ ). The larger is the particle the earlier it arrives to the outlet  
 640 and the lower is its concentration afterwards.

641 The evolution of suspended particle concentration wave is shown in  
 642 Figure 9. Small particles (line 1) are not captured, porous media traps  
 643 intermediate size particles by pore size exclusion mechanism (lines 2 and 3),  
 644 and large particles do not penetrate into porous medium (line 4).





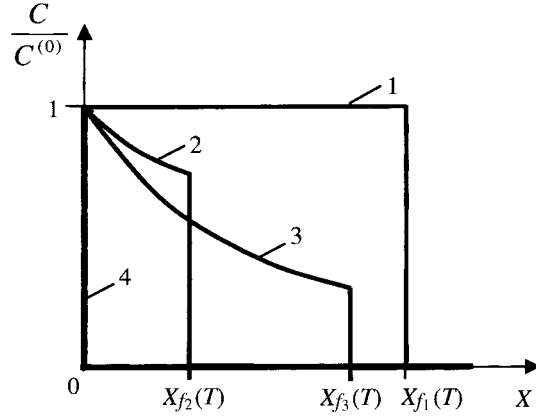


Figure 9. Concentration density profiles for different size particles. Each front moves with the velocity  $\alpha(r_s)/\gamma(r_s)$ . Line 1 corresponds to small particles ( $r_{s1} < r_{pmin}$ ). Lines 2 and 3 are related to intermediate size particles,  $r_{s2} < r_{s3}$ . Line 4 corresponds to large particles ( $r_{s4} > r_{pmax}$ ).

645 In the case where the filtration coefficient is independent of pore radius,  
 646  $\lambda = \lambda(r_s)$ , the explicit formulae (66) and (69) allow solving the inverse problem for determination of the filtration coefficient  $\lambda(r_s)$  from the outlet concentration data of any intermediate size particles:  
 647  
 648

$$649 \quad \lambda(r_s) = \frac{\alpha(r_s)}{1 - \alpha(r_s)} \ln \left( \frac{C^{(0)}(r_s)}{C(r_s, X = 1)} \right). \quad (72)$$

650 6.2. PENETRATION DEPTH

651 The explicit formula (66) allows calculating average penetration depth for  
 652 intermediate size particles into porous media  $\langle X(r_s, T) \rangle$ :

$$653 \quad \langle X(r_s, T) \rangle = \frac{\int_0^{\frac{\alpha}{\gamma}T} X' C(r_s, X', T) dX'}{\int_0^{\frac{\alpha}{\gamma}T} C(r_s, X', T) dX'}. \quad (73)$$

654 Particle concentration density  $C(r_s, X, T)$  is zero ahead of the propagation  
 655 front  $X_f(r_s, T) = \alpha(r_s)/\gamma(r_s)T$  consequently integration in (73) is performed  
 656 from zero to  $[\alpha(r_s)/\gamma(r_s)]T$ . Substituting (66) into (73) and performing the inte-  
 657 gration, we obtain the formula for depth penetration dynamics:

$$658 \quad \langle X(r_s, T) \rangle = \frac{\alpha(r_s)}{\eta(r_s)} \left[ \frac{1 - \exp\left(-\frac{\eta(r_s)}{\gamma(r_s)}T\right) \left(1 + \frac{\eta(r_s)}{\gamma(r_s)}T\right)}{1 - \exp\left(-\frac{\eta(r_s)}{\gamma(r_s)}T\right)} \right]. \quad (74)$$

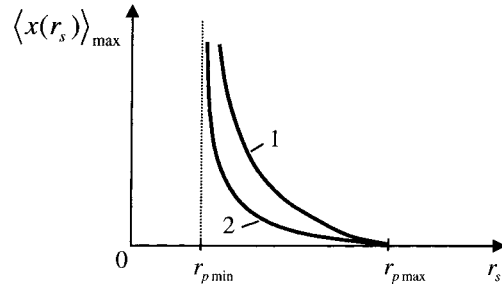


Figure 10. Effect of particle size on penetration depth  $\langle x(r_s) \rangle_{\max}$  for intermediate size particles during filtration in a small pore size variation medium.

659 Tending  $T$  to infinity in (74), we obtain the maximum penetration depth  
 660 for each size particle  $\langle X(r_s) \rangle_{\max}$

$$661 \quad \langle X(r_s) \rangle_{\max} = \frac{\alpha(r_s)}{\eta(r_s)}. \quad (75)$$

662 The penetration depth does not depend on accessibility  $\gamma(r_s)$ . When  
 663 time tends to infinity, the suspended concentration profile given by first  
 664 equation (66) is steady state and is independent of accessibility factor.  
 665 Therefore, the maximum penetration depth is also accessibility-independ-  
 666 ent.

667 For the case where the filtration coefficient is independent of pore  
 668 radius,  $\lambda = \lambda(r_s)$ , substituting (69) into (75), we obtain the following maxi-  
 669 mum penetration depth:

$$670 \quad \langle X(r_s) \rangle = \frac{\alpha}{\lambda(r_s)(1 - \alpha)}. \quad (76)$$

671 Figure 10 shows the maximum penetration depth as a function of par-  
 672 ticle radius. Particles with radii  $r_s = r_{p\max}$  do not penetrate into porous  
 673 media,  $\alpha$  equals zero for this case, and  $\langle X(r_{p\max}) \rangle_{\max} = 0$ . Particles with  
 674 radii  $r_s = r_{p\min}$  flow without being captured. In this case,  $\alpha$  equals unity and  
 675  $\eta(r_s)$  tends to zero; from (75) follows that  $\langle X(r_{p\min}) \rangle_{\max}$  tends to infinity.

676 Curves 1 and 2 in Figure 10 correspond to different filtration coeffi-  
 677 cients,  $\lambda_1 < \lambda_2$ . Particles captured less intensively penetrate deeply.

678 Let us analyse the effect of particle size on penetration depth. The larger  
 679 is the particle, the lower is the flux reduction factor, and the smaller is the  
 680 penetration depth. So, small particles penetrate deeply.

### 681 6.3. AVERAGED CONCENTRATION MODEL

682 In this section we derive an average concentration model and compare it  
 683 with the classical model for deep bed filtration (Iwasaki, 1937).



684 Let us introduce average concentrations for small, intermediate size and  
685 large particles:

$$686 \quad c_1 = \int_0^{r_{p \min}} C(r_s, X, T) dr_s, \quad c_2 = \int_{r_{p \min}}^{r_{p \max}} C(r_s, X, T) dr_s,$$

$$687 \quad c_3 = \int_{r_{p \max}}^{\infty} C(r_s, X, T) dr_s. \quad (77)$$

688 The averaged small particle concentration is obtained by integration of  
689 the first equation (38) over  $r_s$  from zero to  $r_{p \min}$ :

$$690 \quad \frac{\partial c_1}{\partial T} + \frac{\partial c_1}{\partial X} = 0. \quad (78)$$

691 Small particles move with the carrier water velocity without entrapment.  
692 The equations for the total concentration of intermediate size particles  
693 are obtained by integration of first and second equations (63) in  $r_s$  from  
694  $r_{p \min}$  to  $r_{p \max}$ :

$$695 \quad \frac{\partial(\langle \gamma \rangle c_2(X, T))}{\partial T} + \frac{\partial(\langle \alpha \rangle c_2(X, T))}{\partial X} = -\frac{1}{\phi} \frac{\partial \sigma_2(X, T)}{\partial T},$$

$$\frac{\partial \sigma_2(X, T)}{\partial T} = \lambda \phi (1 - \langle \alpha \rangle) c_2(X, T), \quad (79)$$

696 where the averaged flux reduction and accessibility factors are

$$697 \quad \langle \alpha \rangle = \frac{\int_{r_{p \min}}^{r_{p \max}} \alpha(r_s) f_s(r_s, X, T) dr_s}{\int_{r_{p \min}}^{r_{p \max}} f_s(r_s, X, T) dr_s}, \quad (80)$$

$$698 \quad \langle \gamma \rangle = \frac{\int_{r_{p \min}}^{r_{p \max}} \gamma(r_s) f_s(r_s, X, T) dr_s}{\int_{r_{p \min}}^{r_{p \max}} f_s(r_s, X, T) dr_s}. \quad (81)$$

699 The averaged flux reduction and accessibility factors change during par-  
700 ticle retention. The particle retention is described by the deposited con-  
701 centration  $\sigma_2$ . Thus, we close the system (79) introducing constitutive  
702 relations

$$703 \quad \langle \alpha \rangle = \langle \alpha \rangle(\sigma_2) \quad \text{and} \quad \langle \gamma \rangle = \langle \gamma \rangle(\sigma_2). \quad (82)$$

704 If compared with the classical deep bed filtration model (1), the model  
705 (79) for intermediate size particles contains flux reduction term (80) and  
706 accessibility factor (81) in the population balance equation. The capture  
707 rate expression in (79) contains the factor  $(1 - \langle \alpha \rangle)$  showing that the  
708 capture rate should be proportional not to the overall flow velocity  $U$  as



709 it is assumed in (1), but to the fraction of the flow velocity via small pores  
710  $(1 - \langle \alpha \rangle)U$ .

711 The equations for large particle concentrations  $c_3$  and  $\sigma_3$  are obtained  
712 by integration of equations (41) in  $r_s$  from  $r_{p\max}$  to infinity. The averaged  
713 equations are the same as Equations (50) for large particles.

## 714 7. Deep Bed Filtration in a Simple Geometry Medium

715 Let us derive the population balance model for deep bed filtration in a  
716 simplified geometry porous medium, which is a bundle of parallel capillary  
717 alternated by mixing chambers (Figure 2).

718 Particles are assumed to be deposited on sieves;  $\sigma'(x, t)$  is deposited  
719 particle concentration per unit of a sieve area, the vacancy concentration  
720  $h'(x, t)$  is also determined per unit of a sieve area:

$$721 \quad \sigma' = \sigma l, \quad h' = hl. \quad (83)$$

722 The number of particles with radius from the interval  $[r_s, r_s + dr_s]$  cap-  
723 tured in pores with radius from the interval  $[r_p, r_p + dr_p]$  per unit of time  
724 is equal to the number of particles with radius from the interval  $[r_s, r_s +$   
725  $dr_s]$  arriving to the sieve multiplied by water flux via pores with radius the  
726 interval  $[r_p, r_p + dr_p]$ :

$$727 \quad \frac{\partial \sigma'(x, t) f_T(r_s, r_p, x, t)}{\partial t} dr_s dr_p \\ 728 \quad = c(x, t) f_s(r_s, x, t) U \frac{r_p^4 f_p(r_p, x, t)}{\int_0^\infty r_p^4 f_p(r_p, x, t) dr_p} dr_s dr_p. \quad (84)$$

729 Integrating both parts of (84) in  $r_p$  from zero to  $r_s$  and accounting for  
730 (6) result in the expression for the total capture rate of particles with radius  
731  $r_s$  in a single sieve:

$$732 \quad \frac{\partial}{\partial t} (\sigma'(x, t) f_T(r_s, x, t)) = c(x, t) f_s(r_s, x, t) \frac{U \int_0^{r_s} r_p^4 f_p(r_p, x, t) dr_p}{\int_0^\infty r_p^4 f_p(r_p, x, t) dr_p}. \quad (85)$$

733 Changing areal deposited concentration in a sieve per volumetric  
734 deposited concentration (see (83)) and substituting formulae (3), (8) and  
735 (10) in (85), we obtain:

$$736 \quad \frac{\partial \Sigma(r_s, x, t)}{\partial t} = \frac{1}{l} C(r_s, x, t) \frac{U \int_0^{r_s} r_p^4 H(r_p, x, t) dr_p}{\int_0^\infty r_p^4 H(r_p, x, t) dr_p}. \quad (86)$$

737 Comparing formulae (86) and (26), one concludes that the dimensional  
738 filtration coefficient ( $\lambda'$ ) equals the inverse to the distance between the  
739 sieves.



740 It is assumed that in each sieve one particle can plug only one pore, and  
741 vice versa. So, formula (12) can be applied to concentrations in each sieve:

$$742 \quad h'(x, t) f_p(r_p, x, t) = h'_0(x) f_{p0}(r_p, x) - \int_{r_p}^{\infty} \sigma'(x, t) \underline{f_T}(r_s, r_p, x, t) dr_s. \quad (87)$$

743 Differentiating (87) with respect to  $t$  and substituting (84) in the result-  
744 ing equation, we obtain the pore plugging kinetics:

$$745 \quad \frac{\partial}{\partial t} (h'(x, t) f_p(r_p, x, t)) = - \frac{f_p(r_p, x, t) r_p^4}{\int_0^{\infty} f_p(r_p, x, t) r_p^4 dr_p} U c(x, t) \times \\ 746 \quad \times \int_{r_p}^{\infty} f_s(r_s, x, t) dr_s. \quad (88)$$

747 Changing areal vacancy concentration in a sieve per volumetric vacancy  
748 concentration (see (83)) and substituting formulae (3), (8) and (10) in the  
749 resulting equation, we obtain:

$$750 \quad \frac{\partial H(r_p, x, t)}{\partial t} = - \frac{1}{l} \frac{H(r_p, x, t) r_p^4}{\int_0^{\infty} H(r_p, x, t) r_p^4 dr_p} U \int_{r_p}^{\infty} C(r_s, x, t) dr_s. \quad (89)$$

751 The system of governing equations for deep bed filtration ((89) and (86))  
752 in a bundle of parallel capillary alternated by mixing chambers coincide  
753 with the system (28) proposed for a general case of pore space geometry.

754 The dimensional filtration coefficient for deep bed filtration in a bun-  
755 dle of parallel capillary alternated by mixing chambers equals the inverse to  
756 the distance between the sieves, i.e. is constant. It coincides with the pore  
757 plugging kinetics suggested by Sharma and Yortsos (1987a) where  $l$  is con-  
758 sidered to be equal to the pore length.

## 759 8. Conclusions

760 Derivation of the stochastic deep bed filtration model for size exclu-  
761 sion mechanism accounting for particle flux reduction and pore acces-  
762 sibility effects, and analytical solutions obtained allow for the following  
763 conclusions:

- 764 1. Absence of particles in the pores that are smaller than the particles,  
765 results in reduction of the particle carrying water flux if compared with  
766 the overall water flux. It also means that only a fraction of the pore  
767 space is accessible for particles. The flux reduction term appears in the  
768 advection flux in the population balance equation; the accessibility fac-  
769 tor appears in the accumulation term.



- 770 2. The analytical solution for flow in a single pore size  $r'_p$  medium shows  
771 that capture-free advection of small particles ( $r_s < r'_p$ ) takes place, and  
772 large particles ( $r_s > r'_p$ ) do not penetrate into the porous medium. Conse-  
773 quently, there is no deep bed filtration in a uniform pore size medium.  
774 Ignoring flux reduction and accessibility effects results in a separate deep  
775 bed filtration of large different size particles.
- 776 3. The analytical solution for flow in a porous media with small pore size  
777 variation shows that the particles larger than all pores do not move and  
778 that the particles smaller than pores move through the media without  
779 capture.  
780 The intermediate size particles perform deep bed filtration. Populations  
781 with different size particles filtrate independently; the filtration coeffi-  
782 cient and the flux reduction and accessibility factors for each population  
783 are particle-size-dependent.
- 784 4. The larger is the intermediate size particle, the lower is its penetration  
785 depth during deep bed filtration in the rock with small pore size varia-  
786 tion.
- 787 5. The average concentration models can be derived for flow in porous  
788 media with small pore size variation for small particles, for intermediate  
789 size particles and for large particles separately.  
790 The averaged model for intermediate size particles differs from the tradi-  
791 tional deep bed filtration model by the flux reduction and accessibil-  
792 ity factors ( $\langle\alpha\rangle$  and  $\langle\gamma\rangle$ , respectively), that appear in the particle balance  
793 equation. Also, the capture rate in the averaged model is proportional to  
794 the water flux via inaccessible pores, while in the traditional model it is  
795 proportional to the overall water flux.

#### 796 Acknowledgements

797 Authors are mostly grateful to Petrobras colleagues A. G. Siqueira, A. L.  
798 de Souza and F. Shecaira for fruitful and motivating discussions. Many  
799 thanks are due to Prof. A. Shapiro (Denmark Technical University) for the  
800 useful suggestions and improvement of the text.

801 The detailed discussions with Prof. Yannis Yortsos (USC) are highly  
802 acknowledged.

803 Especial gratitude is due to Themis Carageorgos and Poliana Deolindo  
804 (North Fluminense State University UENF, Brazil) for permanent support  
805 and encouragement.

#### 806 References

- 807 Bartelds, G. A., Bruining, J. and Molenaar, J.: 1997, The modeling of velocity enhancement  
808 in polymer flooding, *Transport Porous Media* **26**, 75–88.



- 809 Bedrikovetsky, P., Marchesin, D., Checaira, F., Serra, A. L. and Rezende, E.: 2001, Char-  
810 acterization of deep bed filtration system from laboratory pressure drop measurements,  
811 *J. Petr. Sci. Eng.* **64**(3), 167–177.
- 812 Bedrikovetsky, P., Tran, P., Van den Brock, W. M. G., Marchesin, D., Rezende, E., Siqueira,  
813 A., Serra, A. L. and Shecaira, F.: 2003, Damage characterization of deep bed filtration  
814 from pressure measurements, *J. Soc. Petr. Eng. Prod. Facilities*, **3**, 119–128.
- 815 Dawson, R. and Lantz R. B.: 1972, Inaccessible pore volume in polymer flooding, *Soc. Petr.*  
816 *Eng. J.* 448–452, October.
- 817 Elimelech, G., Gregory, J., Jia, X. and Williams, R. A.: 1995, *Particle Deposition and Aggre-*  
818 *gation*, Butterworth-Heinemann, USA.
- 819 Herzig, J. P., Leclerc, D. M. and Goff, P. le.: 1970, Flow of suspensions through porous  
820 media – application to deep filtration, *Ind. Eng. Chem.* **62**(5), 8–35.
- 821 Iwasaki, T.: 1937, Some notes on sand filtration, *J. Am. Water Works Ass.* 1591–1602.
- 822 Khatib, Z. I.: 1994, Prediction of Formation Damage Due to Suspended Solids: Modeling  
823 Approach of Filter Cake Buildup in Injectors, 1995, SPE paper 28488 presented at SPE  
824 66th Annual Technical Conference and Exhibition held in New Orleans, LA, USA, 25–  
825 28 September
- 826 Khilar, K. and Fogler, S.: 1998, *Migration of Fines in Porous Media*, Kluwer Academic Pub-  
827 lishers, Dordrecht/London/Boston.
- 828 Landau, L. D. and Lifshitz, E. M.: 1980, *Statistical Physics (Course on Theoretical Physics,*  
829 *V.5)*, 3rd edition, Pergamon Press, Oxford, UK.
- 830 Landau, L. D. and Lifshitz, E. M.: 1987, *Fluid Mechanics (Course on Theoretical Physics,*  
831 *V.6)*, 2nd edition, Pergamon Press, Oxford, UK.
- 832 Massei, N., Lacroix, M., Wang, H. Q. and Dupont, J.: 2002, Transport of particulate mater-  
833 ial and dissolved tracer in a highly permeable porous medium: comparison of the trans-  
834 fer parameters, *J. Contam. Hydro.* **57**, 21–39.
- 835 Oort, E. V., Velzen, J. F. G. V. and Leerlooijer, K.: 1993, Impairment by Suspended Solids  
836 Invasion: Testing and Prediction, *SPE paper* **23822**.
- 837 Pang, S. and Sharma, M. M.: 1994, A Model for Predicting Injectivity Decline in Water  
838 Injection Wells. *SPE paper* **28489**, 275–284.
- 839 Payatakes, A. C., Tien, C. and Turian, R. M.: 1973, A new model for granular porous  
840 media. I. model formulation, *AIChE J.*, **19**(1), 58–76.
- 841 Payatakes, A. S., Rajagopalan, R. and Tien, C.: 1974, Application of porous medium models  
842 to the study of deep bed filtration, *The Canadian J. Chem. Eng.* **52**.
- 843 Rege, S. D. and Fogler, H. S.: 1988, A network model for deep bed filtration of solid par-  
844 ticles and emulsion drops, *AIChE J.* **34**(11), 1761–1772.
- 845 Sahimi, M. and Imdakm, A. O.: 1991, Hydrodynamics of particulate motion in porous  
846 media. *Phys. Rev. Letters* **66**(9), 1169–1172.
- 847 Seljakov, V. I. and Kadet, V. V.: 1996, *Percolation Models in Porous Media*, Kluwer  
848 Academic, Dordrecht-NY-London.
- 849 Sharma, M. M. and Yortsos, Y. C.: 1987a, Transport of particulate suspensions in porous  
850 media: model formulation, *AIChE J.* **33**(10), 1636.
- 851 Sharma, M. M. and Yortsos, Y. C.: 1987b, A network model for deep bed filtration pro-  
852 cesses, *AIChE J.* **33**(10), 1644–1653.
- 853 Sharma, M. M. and Yortsos, Y. C.: 1987c, Fines migration in porous media, *AIChE J.*  
854 **33**(10), 1654–1662.
- 855 Siqueira, A. G., Bonet, E. and Shecaira, F. S.: 2003, Network modelling for transport of  
856 water with particles in porous media. *SPE paper* 18257 presented at the SPE Latin Amer-  
857 ican and Caribbean Petroleum Engineering Conference held in Port-of-Spain, Trinidad  
858 and Tobago.



- 859 Tikhonov, A. N. and Samarskii, A. A.: 1990, *Equations of Mathematical Physics*, Dover,  
860 New York.
- 861 Veerapen, J. P., Nicot, B. and Chauveteau, G. A.: 2001, In-Depth Permeability Damage by  
862 Particle Deposition at High Flow Rates, SPE paper 68962 presented at presented at the  
863 SPE European Formation Damage Conference to be held in The Hague, The Netherlands  
864 21–22 May 2001.
- 865 Wennberg, K. E. and Sharma, M. M.: 1997, Determination of the filtration coefficient and  
866 the transition time for water injection, *SPE* **38181**, 353–364.

Uncorrected Proof

